

## Spectral modulation of ultraviolet femtosecond laser pulse by molecular alignment of CO<sub>2</sub>, O<sub>2</sub>, and N<sub>2</sub>

Yongdong Wang, Xiaomin Dai, Jian Wu, Liang'en Ding,<sup>a)</sup> and Heping Zeng

State Key Laboratory of Precision Spectroscopy, East China Normal University, Shanghai 200062, China

(Received 3 August 2009; accepted 21 December 2009; published online 20 January 2010)

We demonstrate efficient third harmonic generation of a near infrared femtosecond pulse through cascaded frequency doubling and sum-frequency generation processes, where the group velocity mismatching between the involved fundamental and generated second harmonic pulses, before they are sent to frequency mixing, are precompensated with a properly inserted nonlinear crystal. The spectrum of the generated third harmonic pulse with energy of 1.1 mJ is further modulated by using impulsive molecular alignments of CO<sub>2</sub>, O<sub>2</sub>, and N<sub>2</sub>, where significantly broadened spectrum in the ultraviolet spectral region is observed due to the additional cross-focusing effect from the parallel aligned molecules and the consequently enhanced self-phase modulation. © 2010 American Institute of Physics. [doi:10.1063/1.3292017]

Nonlinear frequency conversion, such as third harmonic (TH) generation of infrared femtosecond pulse, is an efficient approach to obtain ultrashort laser pulse in the ultraviolet spectral region.<sup>1-3</sup> As compared to the relatively small third-order nonlinearities of the gaseous media,<sup>4,5</sup> the cascaded second-order frequency mixing processes in the quadratic nonlinear crystals shows a efficiency for TH generation, where the residual fundamental (FW) pulse is mixed with the generated second-harmonic (SH) one.<sup>6-9</sup> However, for ultrashort laser pulses, the larger light dispersion in the crystal limits the available energy conversion efficiency and the spectral bandwidth of the generated TH pulse.<sup>10</sup> In this letter, we show that the group velocity mismatching (GVM) between the residual FW and the generated SH pulses can be compensated well by using a properly inserted nonlinear crystal, which thus increases the TH generation efficiency through the sum-frequency generation in the third nonlinear crystal. The limited bandwidth of the generated intense TH pulse is further significantly broadened by propagating it in prealigned molecular gases, resulting from the additional cross-focusing effect of the parallel aligned molecules and the sequentially enhanced self-phase modulation (SPM).

Experimentally, as schematically illustrated in Fig. 1, an output from a Ti:Sapphire amplified laser system (800 nm, 70 fs, and 10 Hz) was first sent to generate TH pulse through cascaded second-order nonlinear frequency mixing, and then the residual FW pulse was used to prealign the molecular gases for spectral modulation of the generated TH pulse. Throughout this letter, we label the FW pulse used for molecular alignment and the generated TH pulse as the pump and probe pulses, respectively. The pulse energies of the pump and probe pulses were measured to be 7.0 and 1.1 mJ, respectively. In order to efficiently generate TH pulse, three  $\beta$ -BaB<sub>2</sub>O<sub>4</sub> (BBO) crystals were sequentially used as follows: the first BBO crystal (BBO-1, 200  $\mu$ m thick, 29.2°-cut, type-I) was used for frequency doubling; the GVM between the generated SH and the residual FW pulses was compensated by using the second BBO crystal (BBO-2, 200  $\mu$ m thick, 29.2°-cut) whose crystallographic axis was

rotated by 45° with respect to BBO-1; TH pulse was then produced in the third BBO crystal (BBO-3, 200  $\mu$ m thick, 44.3°-cut, type-I) through frequency summing of the FW and SH pulses. The FW and generated TH pulses were focused by two separated concave mirrors ( $f=100$  cm). After combined collinearly with a dichromatic mirror (DM), the FW and TH pulses were then steered into a 100 cm long gas cell, which was filled with pure CO<sub>2</sub>, O<sub>2</sub>, or N<sub>2</sub> at a gas pressure of 2 atm. The time delay of the probe TH pulse with respect to the pump FW pulse is tuned by using a motorizing stage in the probe arm, so as to properly match the molecular alignment revivals. After separation from the FW pulse with high reflective mirrors at TH central wavelength, the output spectra of the TH pulse after the gas cell were monitored by using a spectrometer.

Due to the light dispersion of the BBO crystal, as characterized by GVM between them, the p-polarized FW pulse and the generated s-polarized SH pulse propagate at different group velocities, leading to limited energy conversion efficiency of the sequential frequency mixing process for TH generation. By inserting an additional BBO crystal with properly rotated crystallographic axis with respect to the frequency doubling one, the induced time lag between the FW and SH pulses can be partly compensated. Here, assisted by a 200  $\mu$ m thick crystal of BBO-2 with its crystallographic

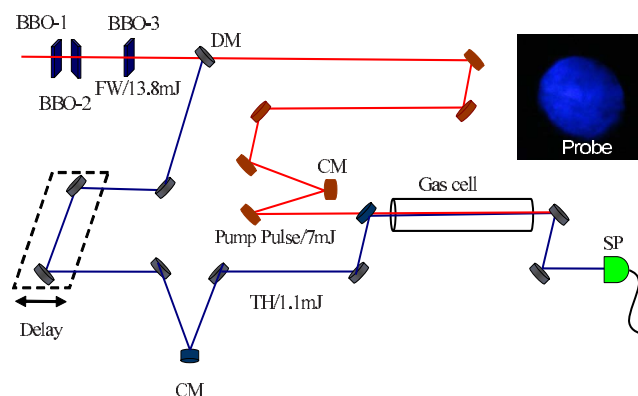


FIG. 1. (Color online) Schematic illustration of the experimental setup. DM: dichromatic mirror, CM: concave mirror, SP: spectrometer. The inset shows the output spatial profile of the TH pulse without pump.

<sup>a)</sup>Electronic mail: leding@phy.ecnu.edu.cn.

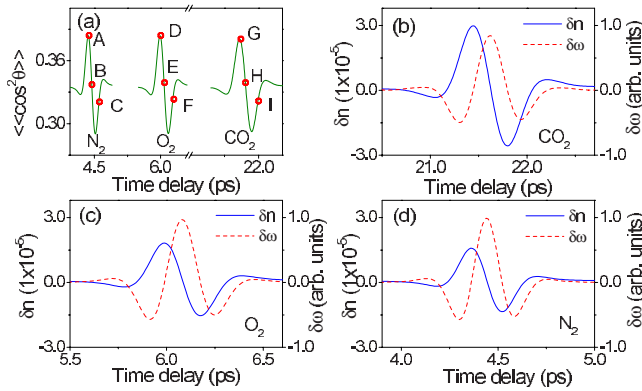


FIG. 2. (Color online) (a) Calculated molecular alignment signals, and corresponding refractive index variations and induced spectral shifts around the half-revival times of molecular (b)  $CO_2$ , (c)  $O_2$ , and (d)  $N_2$ .

axis was rotated by  $45^\circ$  with respect to the BBO-1, the time lag between the FW and SH pulses is compensated from 100 to 33 fs. Consequently, driving by a FW pulse of 13.8 mJ, TH pulse of 1.1 mJ is with an energy conversion efficiency of 8% was produced as compared to 5% for the case without the GVM compensation crystal. The duration of the TH pulse is measured to be about 70 fs. In general, the 6% TH generation efficiency was achieved with sequential crystals.<sup>11–13</sup> Recently, a TH generation efficiency of 8% was demonstrated by using two sequential crystals at a noncollinear scheme with a pulse duration of about 100 fs.<sup>2</sup>

In order to further broaden the spectrum of the energetic TH pulse to produce spectra capable of supporting few-cycle laser pulses in ultraviolet region, we then propagate it in prealigned molecules and take advantage of the cross-phase modulation produced by the molecular alignment. Differing from the atomic gas, the molecules are periodically oriented after the termination of the ultrashort pump pulse, which provides us an efficient approach to control the propagation dynamics of the succeeding ultrashort probe pulse.<sup>14,15</sup> The additional refractive index change originated from the molecular alignment read as<sup>11</sup>  $\delta n(r, t) = 2\pi(\rho_0\Delta\alpha/n_0) \times [\langle\langle\cos^2\theta\rangle\rangle(r, t) - 1/3]$ , where  $\rho_0$  is the initial molecular density,  $\Delta\alpha = \alpha_{\parallel} - \alpha_{\perp}$  is the polarizability difference between the components parallel and perpendicular to the molecular axis,  $n_0$  is the linear refractive index. The molecular alignment is characterized by  $\langle\langle\cos^2\theta\rangle\rangle$ ,<sup>16</sup> where  $\theta$  is the angle between the molecular axis and the field polarization of the probe pulse. Figure 2(a) shows the calculated molecular alignment metrics  $\langle\langle\cos^2\theta\rangle\rangle$  around the half revival time of  $N_2$ ,  $O_2$ , and  $CO_2$  molecules, which are, respectively, greater and smaller than 1/3 for parallel and perpendicular orientations. As shown in Figs. 2(b)–2(d) (solid curves), depending on the molecules are oriented parallel and perpendicular to the probe polarization, the refractive indices are increased and decreased, respectively. Since the molecular alignment is more significant at the beam center than its periphery, an additional cross-(de)focusing effect<sup>15</sup> is hence introduced to the probe pulse as it is delayed to experience various molecular alignment revivals. It is similar to the molecular alignment assisted supercontinuum generation.<sup>17,18</sup> Meanwhile, the time dependent refractive index variation of the prealigned molecules also introduces a frequency shift<sup>15</sup> of  $\delta\omega(t) = -\partial\varphi_m/\partial t \sim -\partial\delta n(t)/\partial t$  to the probe pulse, as shown in Figs. 2(b)–2(d) (dashed curves). The spectrum of the probe

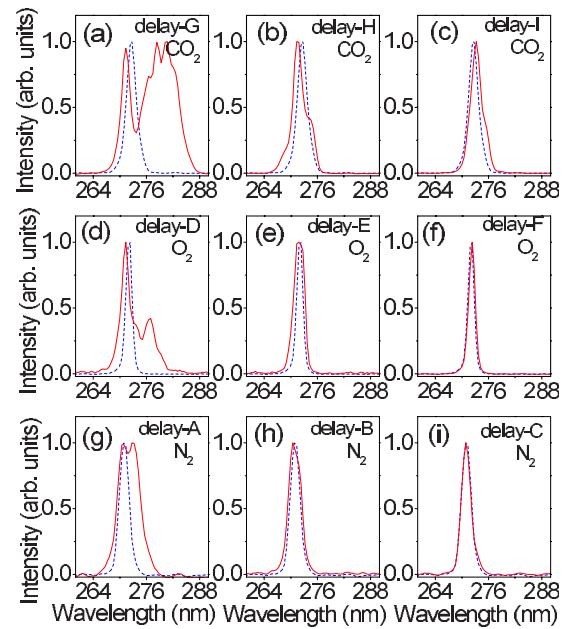


FIG. 3. (Color online) Measured output spectra of the probe pulses at various molecular alignment revivals of [(a)–(c)]  $CO_2$ , [(d)–(f)]  $O_2$ , and [(g)–(i)]  $N_2$  as labeled in Fig. 2. The solid and dashed curves represent the spectra of the probe pulse when the molecular alignment is turned on and turned off, respectively.

pulse is expected to be red or blue shifted when it is tuned to match the regions of positive and negative slope of the molecular alignment revival, respectively. Such time dependent frequency shift was recently demonstrated to tune the central wavelength of few-cycle laser pulse.<sup>19</sup>

In our experiment, as shown in Fig. 1, the molecules inside the gas cell were first prealigned through impulsive rotational Raman excitation of an intense FW pump pulse. As shown in Fig. 3(a), the spectrum of the TH pulse is significantly broadened with respect to the random orientation case when it was tuned to the parallel revival of molecular  $CO_2$  [delay-G as labeled in Fig. 2(a)]. Both redshifted and blueshifted frequency components are generated, leading to a spectral bandwidth of  $\sim 13$  nm (FWHM) around 276 nm, which is 6.5 times of the initial spectral width of 2 nm. As the temporal peak of the probe pulse is delayed to delay-G, the pulse lead and tail experience the regions of positive and negative slope of the molecular alignment revival, respectively, leading to the generation of redshifted and blueshifted frequency components. Such spectral modulation is expected to be more significant at delay-H as indicated in Fig. 2(a). As shown in Fig. 3(b), the spectrum of the TH probe pulse is modulated to be blueshifted as predicted by the time-dependent nonlinear phase accumulation, while the spectral bandwidth is much narrower than that at delay-G. We, therefore, attribute that the cross-focusing effect from the parallel molecular alignment revival and the consequently enhanced SPM process contribute importantly for the observed spectral broadening of the TH probe pulse at delay-G, which is consistent with the recent demonstration on the controllable supercontinuum generation.<sup>17,18</sup> For the perpendicular molecular alignment revival with additional cross-defocusing effect, the SPM process is expected to be weakened. As shown in Fig. 3(c) for delay-I, during the positive slope of the molecular alignment revival, the spectrum of the TH probe is somewhat redshifted with quite small spectral broadening. The

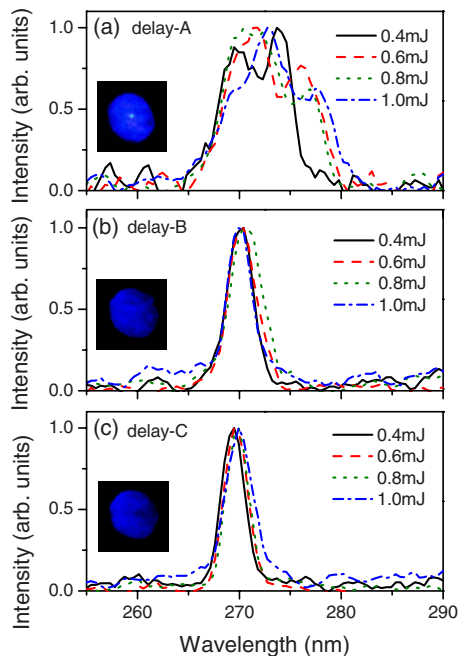


FIG. 4. (Color online) The output spectra of the TH pulse vs its input energy when it is tuned to match various molecular alignment revivals of  $N_2$ . The insets show the output spatial profiles of the TH pulse at an input energy of 1 mJ.

GVM induced walkoff between the FW and TH pulses over the interaction region was estimated to be about 10 fs, which is fairly small as compared with the molecular alignment cycle and no significant influence on our experimental measurements is expected.

The molecular alignment induced spectral modulation experiments of the TH probe pulse were also performed in molecular  $O_2$  and  $N_2$  with the same condition. With respect to molecular  $CO_2$ , as shown in Figs. 2(c) and 2(d), the additional refractive index variations of the molecular  $O_2$  and  $N_2$ , proportional to the polarizability difference  $\Delta\alpha$ ,<sup>20–22</sup> are relatively smaller, which correspond to weakened influences of the cross-focusing effect and the subsequent SPM process. Therefore, as shown in Figs. 3(e) and 3(h), for the parallel revivals of the molecular alignment of  $O_2$  and  $N_2$  at delays D and A, the spectral broadening of the TH probe pulse is smaller, than for the parallel molecular alignment revival of  $CO_2$  at delay-G. As shown in Figs. 3(d)–3(i), the spectral modulation owing to the accumulated time-dependent nonlinear phase shift is also correspondingly weakened at other molecular alignment revivals of molecular  $O_2$  and  $N_2$  due to their relatively smaller polarizability differences.

It is the cross-focusing effect from the parallel revival of the molecular alignment and the subsequently enhanced SPM process that leads to the observed spectral broadening of the probe pulse in our experiment. This was further confirmed by studying the output spectral and spatial profiles of the TH pulse at various input energies as shown in Fig. 4. As compared with the case of without pump pulse (see the inset

of Fig. 1), an intense core is observed at the beam center as shown in the inset of Fig. 4(a), indicating filamentation dynamics of the TH pulse due to the presence of the cross-focusing effect. The TH spectra were correspondingly broadened as shown in Fig. 4(a), which weakly depended on the probe pulse energy. In the absence of cross-focusing of the molecular alignment, as shown in Figs. 4(b) and 4(c), no spectral broadening was observed due to the weak SPM processes without filamentation [see the insets of Figs. 4(b) and 4(c) for the output spatial profiles] which is similar to the individual propagation of the TH pulse. Therefore, the cross-focusing effect is very important to enhance the subsequent SPM process for the observed spectral broadening of the TH pulse in our experiments.

In summary, based on the GVM compensated cascaded second-order nonlinear frequency mixing processes for energetic TH pulse generation and the consequent molecular alignment revival for spectral modulation, we demonstrated that the energetic broadband ultraviolet laser pulse with pulse energy of 1.1 mJ and spectral bandwidth of 13 nm (FWHM) can be generated.

This project was funded by the National Basic Research Program of China (Grant No. 2006CB06001), the Program for Chingjiang and Innovative Research Team in University; Shanghai Academic Discipline Project (Grant No. B408).

- <sup>1</sup>S. Backus, J. Peatross, Z. Zeek, A. Rundquist, G. Taft, M. M. Murnane, and H. C. Kapteyn, *Opt. Lett.* **21**, 665 (1996).
- <sup>2</sup>S. Cialdi, M. Petrarca, and C. Vicario, *Opt. Lett.* **31**, 2885 (2006).
- <sup>3</sup>S. Suntsov, D. Abdollahpour, D. G. Papazoglou, and S. Tzortzakakis, *Opt. Express* **17**, 3190 (2009).
- <sup>4</sup>C. G. Durfee III, S. Backus, H. C. Kapteyn, and M. M. Murnane, *Opt. Lett.* **24**, 697 (1999).
- <sup>5</sup>T. Fuji, T. Horio, and T. Suzuki, *Opt. Lett.* **32**, 2481 (2007).
- <sup>6</sup>R. J. Gehr, M. W. Kimmel, and A. V. Smith, *Opt. Lett.* **23**, 1298 (1998).
- <sup>7</sup>M. Aoyama, T. Harimoto, J. Ma, Y. Akahane, and K. Yamakawa, *Opt. Express* **9**, 579 (2001).
- <sup>8</sup>P. Baum, S. Lochbrunner, and E. Riedle, *Appl. Phys. B: Lasers Opt.* **79**, 1027 (2004).
- <sup>9</sup>A. E. Jaiilaubekov and S. E. Bradforth, *Appl. Phys. Lett.* **87**, 021107 (2005).
- <sup>10</sup>Y. Liu, J. C. Diels, and S. Member, *IEEE J. Quantum Electron.* **42**, 760 (2006).
- <sup>11</sup>A. M. Weiner, A. M. Kanan, and D. E. Leaird, *Opt. Lett.* **23**, 1441 (1998).
- <sup>12</sup>A. Dubietis, G. Tamosauskas, and A. Varanavicius, *Opt. Commun.* **186**, 211 (2000).
- <sup>13</sup>M. Ghotbi, M. Ebrahim-Zadeh, A. Majchrowski, E. Michalski, and I. V. Kityk, *Opt. Lett.* **29**, 2530 (2004).
- <sup>14</sup>H. Cai, J. Wu, A. Couairon, and H. Zeng, *Opt. Lett.* **34**, 827 (2009).
- <sup>15</sup>J. Wu, H. Cai, H. Zeng, and A. Couairon, *Opt. Lett.* **33**, 2593 (2008).
- <sup>16</sup>H. Stapelfeldt and T. Seideman, *Rev. Mod. Phys.* **75**, 543 (2003).
- <sup>17</sup>H. Cai, J. Wu, Y. Peng, and H. Zeng, *Opt. Express* **17**, 5822 (2009).
- <sup>18</sup>J. Wu, H. Cai, Y. Peng, and H. Zeng, *Phys. Rev. A* **79**, 041404(R) (2009).
- <sup>19</sup>J. Wu, H. Cai, A. Couairon, and H. Zeng, *Phys. Rev. A* **79**, 063812 (2009).
- <sup>20</sup>R. A. Bartels, T. C. Weinacht, N. Wagner, M. Baertschy, H. C. Greene, M. M. Murnane, and H. C. Kapteyn, *Phys. Rev. Lett.* **88**, 013903 (2001).
- <sup>21</sup>M. Spanner, Ph.D. thesis, Waterloo University, 2004.
- <sup>22</sup>F. Calegari, C. Vozzi, S. Gasilov, E. Benedetti, G. Sansone, M. Nisoli, S. De Silvestri, and S. Stagira, *Phys. Rev. Lett.* **100**, 123006 (2008).